

# A theoretical model of the femtosecond laser ablation of semiconductors considering inverse bremsstrahlung absorption

Lin Xiaohui(林晓辉)<sup>1,†</sup>, Zhang Chibin(张赤斌)<sup>1</sup>, Ren Weisong(任维松)<sup>1</sup>, Jiang Shuyun(蒋书运)<sup>1</sup>, and Ouyang Quanhui(欧阳全会)<sup>2</sup>

<sup>1</sup>School of Mechanical Engineering, Southeast University, Nanjing 211189, China

<sup>2</sup>Wuhan Technical College of Communication, Wuhan 430062, China

**Abstract:** The mechanism of the femtosecond laser ablation of semiconductors is investigated. The collision process of free electrons in a conduction band is depicted by the test particle method, and a theoretical model of nonequilibrium electron transport on the femtosecond timescale is proposed based on the Fokker–Planck equation. This model considers the impact of inverse bremsstrahlung on the laser absorption coefficient, and gives the expressions of electron drift and diffusion coefficients in the presence of screened Coulomb potential. Numerical simulations are conducted to obtain the nonequilibrium distribution function of the electrons. The femtosecond laser ablation thresholds are then calculated accordingly, and the results are in good agreement with the experimental results. This is followed by a discussion on the impact of laser parameters on the ablation of semiconductors.

**Key words:** femtosecond laser; nonequilibrium distribution; inverse bremsstrahlung absorption; ablation mechanism

**DOI:** 10.1088/1674-4926/33/4/046002

**EEACC:** 2520

## 1. Introduction

In the process of femtosecond laser processing, extremely high energy can be transferred to materials in a very short time duration, which causes the ablation of materials in the irradiated area. The electrons in the valence band can obtain energy by absorbing photons and then turn into free electrons in the conduction band. It has been experimentally verified that in femtosecond laser processing, electrons are in a nonequilibrium state, which could be attributed to the ultra short pulse durations<sup>[1,2]</sup>.

How to describe the electron configuration in semiconductors is key to modeling the mechanisms of semiconductor ablation via ultra-short pulses. A two-temperature model is proposed to describe the time evolution of electron and phonon distributions, which has been utilized by many researchers to study the ablation mechanisms of materials via femtosecond lasers<sup>[3–8]</sup>. The model is appropriate under the condition that both electrons and photons are in an equilibrium state. While for femtosecond lasers, the pulse widths are of the order of a femtosecond and the electrons are in a nonequilibrium state, therefore the so-called electron temperature has no meaning. As a result, the two-temperature model cannot be applied. Instead, electron transport during the ablation of semiconductors by femtosecond pulses can be depicted by the kinetic models based on nonequilibrium transport theory. The Boltzmann equation is a method commonly used for describing the time evolution of electrons<sup>[9–14]</sup>. Rethfeld *et al.* presented a model to describe the time evolution of electron distributions in metals under femtosecond laser irradiation using the Boltzmann equation<sup>[13]</sup>, and it was found

that for lasers with pulse durations less than  $10^{-13}$  s, the electron distributions noticeably deviated from the equilibrium state. It was also confirmed that free electrons are in a nonequilibrium state during the ablation of dielectrics by femtosecond pulses by Kaiser *et al.*, who studied the energy transfer in dielectric ablation based on the Boltzmann equation<sup>[12]</sup>.

Since the Boltzmann equation is a multidimensional nonlinear differential-integral equation, it is difficult to solve it numerically. An alternative is the stochastic model based on Brownian motion. The time evolution of nonequilibrium electron distributions can be described by the Fokker–Planck equation. The Fokker–Planck equation is equivalent to the Boltzmann equation, which is a differential equation, and is easier to solve when compared with the Boltzmann equation. Some researchers applied the same form of the linear Fokker–Planck equation to study the ablation mechanisms of dielectrics by femtosecond lasers<sup>[15–18]</sup>. In these studies, the relaxation time of the electrons and laser absorption coefficient are assumed to be constant. But the relaxation time and absorption coefficient are actually not constant; instead, they are related to the microstate of electrons.

This paper uses the mechanism of screened Coulomb collision to describe the electron–electron collisions. The laser energy reduction resulting from the inverse bremsstrahlung absorption is taken into account. Using the test particle method, a nonlinear Fokker–Planck model is developed to depict the distribution functions of the free electrons. A physical image of this model can better reflect the time evolution of the nonequilibrium electrons in materials under femtosecond laser pulses.

† Corresponding author. Email: lxh60@yahoo.com.cn

Received 19 August 2011, revised manuscript received 22 December 2011

© 2012 Chinese Institute of Electronics

## 2. Theoretical model

### 2.1. Time evolution of nonequilibrium electron distribution

When target materials are under the irradiation of femtosecond laser pulses, the electrons in the valence band can jump into the conduction band to become free electrons, as a result of the mechanisms of multiphoton ionization and avalanche ionization. The collision process of free electrons in the conduction band can be described by the test particle method, which requires that screened Coulomb collisions are generated between a test electron beam and nonequilibrium electrons. The distribution of free electrons is assumed to be isotropic. Let  $f(v, t)$  represent the probability distribution function of the velocity of nonequilibrium electrons at time  $t$ , which can be described as follows using the Fokker–Planck equation expressed by the Rosenbluth potential function:

$$\begin{aligned} \frac{\partial f(v, t)}{\partial t} + \frac{q_e E(t) v^2}{m_e} \frac{\partial}{\partial v} \left( \frac{1}{v^2} f(v, t) \right) \\ = -\Gamma v^2 \frac{\partial}{\partial v} \left( \frac{1}{v^2} \frac{\partial H(v)}{\partial v} f(v, t) \right) \\ + \frac{\Gamma v^2}{2} \frac{\partial^2}{\partial v^2} \left( \frac{1}{v^2} \frac{\partial^2 G(v)}{\partial v^2} f(v, t) \right) + (S_1 + S_2), \end{aligned} \quad (1)$$

where  $\Gamma = \frac{4\pi e^4}{m_e^2 \epsilon_0^2} \ln \Lambda$ , in which  $e$  is the electric charge,  $m_e$  is the electron mass,  $\epsilon_0$  is the permittivity of materials, and  $\ln \Lambda$  is the Coulomb logarithm.  $S_1$  is the multiphoton ionization rate, given by the Keldysh’s formula  $S_1 = \frac{2\omega}{9\pi N_e} \left( \frac{m_e \omega}{\hbar} \right)^{\frac{3}{2}} \varphi \left( \sqrt{2k - \frac{2U_L}{\hbar \omega}} \right) \times \exp \left( 2k \left( 1 - \frac{1}{4r^2} \right) \right) \times \left( \frac{1}{16r^2} \right)^k$ , where  $\omega$  represents the laser frequency,  $\hbar$  is the reduced Planck constant,  $k$  is the number of absorbed photons,  $U_L$  is the band gap energy, and  $r$  is calculated by  $r = \frac{\omega \sqrt{m_e U_L}}{q_e E}$  [20].  $S_2$  is the avalanche ionization rate given by  $S_2 = \alpha I(t) f(v, t)$ , where  $\alpha$  denotes the avalanche ionization coefficient,  $E$  is the electric field strength, and  $I(t)$  is the laser intensity at  $t$  time [19].  $H(v)$  and  $G(v)$  in Eq. (1) are the Rosenbluth potential functions expressed by

$$H(v) = \frac{8\pi N_e}{C} \int_0^\infty \frac{f(v_1, t) dv_1}{v - v_1}, \quad (2)$$

and

$$G(v) = \frac{4\pi N_e}{C} \int_0^\infty f(v, t) (v - v_1) dv_1, \quad (3)$$

respectively, in which  $N_e$  represents the average number density of electrons and  $C$  is the speed of light.

Let  $t = -\infty$  be the initial time. Thus, the initial condition of Eq. (1) can be expressed as

$$f(v, t)_{t=-\infty} = 0, \quad (4)$$

which implies that there is no free electron in the conduction band at the beginning.

The boundary conditions for velocity space are described by

$$J(v, t)_{v=0} = 0, \quad (5)$$

and

$$f(v, t)_{v=\infty} = 0, \quad (6)$$

where  $J(v, t)$  represents the probability flux of electrons given by

$$J(v, t) = \Gamma \left[ \frac{1}{v^2} \frac{\partial H(v)}{\partial v} f(v, t) - \frac{1}{2} \frac{1}{v^2} \frac{\partial^2 G(v)}{\partial v^2} f(v, t) \right]. \quad (7)$$

Equation (5) ensures that once an excited electron becomes a free electron in the conduction band, it will never fall back to the valence band, which might be caused by the impact of electron recombination. Equation (6) guarantees that the velocity of free electrons cannot exceed the speed of light. The time evolution of electron distribution functions can be derived by solving the nonlinear partial differential equations consisting of Eqs. (1) to (7).

### 2.2. Numerical solution

After the dimensionless of Eq. (1), the Runge–Kutta method can be applied to solve the time step of this equation, which is separated by a finite difference at each step. Then, the resulting nonlinear equations can be solved by the overrelaxation iterative method to achieve the probability function of electrons that satisfies the accuracy requirement.

The difficulty of solving this nonlinear equation lies in how to calculate the dimensionless quantities  $H^*(v^*)$  and  $G^*(v^*)$ , since they are integrals of unknown function  $f(v^*)$ . Also,  $H^*(v^*)$  is singular at the point  $v_1^* = v^*$ . Conventional numerical integration methods can hardly be used to effectively solve the problem for the following reasons: first, the integral on an interval containing a singular point cannot be performed; second, one extra global integration on the singular point for each  $f(v_1^*)$  required in the iteration process leads to a great amount of computation.

Consider the distribution function  $f(v_j^*)$  at each node point obtained after each iteration. Suppose the velocity of electrons in each small range of  $[v_j^*, v_j^* + \Delta v^*]$  is uniformly distributed. The values of  $H^*(v^*)$  and  $G^*(v^*)$  at the node point can be expressed by

$$H^*(v_i^*) = \sum_{j=1}^n C_{i,j} f(v_j^*), \quad \forall i, j = 1, 2, \dots, n, \quad (8)$$

and

$$G^*(v_i^*) = \sum_{j=1}^n D_{i,j} f(v_j^*), \quad \forall i, j = 1, 2, \dots, n, \quad (9)$$

where  $i$  and  $j$  are indices of discrete nodes.

The element  $C_{i,j}$  is defined by  $C_{i,j} = 8\pi \int_{v_{j-\frac{1}{2}}^*}^{v_{j+\frac{1}{2}}^*} \frac{dv_1^*}{v_i^* - v_1^*}$  and the element  $D_{i,j}$  is defined by  $D_{i,j} = 4\pi \int_{v_{j-\frac{1}{2}}^*}^{v_{j+\frac{1}{2}}^*} (v_i^* - v_1^*) dv_1^*$ , where  $v_{j+\frac{1}{2}}^* = \frac{1}{2} (v_j^* + v_{j+1}^*)$ ,  $v_{j-\frac{1}{2}}^* = \frac{1}{2} (v_j^* + v_{j-1}^*)$ .

$$\text{And: } C_{i,j} = -8\pi \left[ \ln \left( v_i^* - v_{j+\frac{1}{2}}^* \right) - \ln \left( v_i^* - v_{j-\frac{1}{2}}^* \right) \right],$$

$$\text{and } D_{i,j} = -2\pi \left[ \left( v_i^* - v_{j+\frac{1}{2}}^* \right)^2 - \left( v_i^* - v_{j-\frac{1}{2}}^* \right)^2 \right].$$

Therefore, the values of  $H^{*(k+1)}(v_i^*)$  and  $G^{*(k+1)}(v_i^*)$  at the  $(k+1)$ th iteration can be obtained by the linear addition of  $f^{(k)}(v_j^*)$ ,  $H^{*(k)}(v_j^*)$ , and  $G^{*(k)}(v_j^*)$  at the  $k$ th iteration with Eqs. (8) and (9). This way can not only eliminate the requirement of performing integrations containing singular points, but also significantly reduces the computations for  $H^*(v_i^*)$  and  $G^*(v_i^*)$ .

### 3. Calculations of threshold damage fluence, laser absorption coefficient and relaxation time

#### 3.1. Threshold damage fluence

When the number density of free electrons in the conduction band reaches a critical value, material ablation can occur. Assume that the nondimensional form of the number density of free electrons in the conduction band at time  $t^*$  represented by  $n^*(t^*)$ , can be derived as  $n^*(t^*) = \frac{n(t)}{N_c} = \int_0^\infty f(v^*, t^*) dv^*$ . The ablation criteria can be described as

$$n^*(t^*) = n_c^*, \quad (10)$$

where  $n_c^* = n_c/N_c$ , here  $n_c$  denotes the critical number density of free electrons while ablation occurs.

The time  $t^*$  at which ablation occurs can be calculated based on Eq. (10) by interpolation. The nondimensional form of threshold damage fluence can be expressed as  $F_c^* = \frac{F_c}{I_{\max} t_p} = \int_0^{t_c^*} I^*(t^*) dt^*$ .

#### 3.2. The laser absorption coefficient

The laser energy is reduced because free electrons can absorb the energy of photons by inverse bremsstrahlung absorption. Assume the damping rate of femtosecond laser energy is denoted by  $\gamma$ , then the laser power density at time  $t$ ,  $w(t)$ , can be expressed as  $w(t) = w_0 e^{-\gamma t}$ , where  $w_0$  is the power density at the initial time expressed as  $w_0 = \varepsilon_0 E_0^2/2$ . Here  $E_0$  represents the strength of the electric field at the initial time. So the laser power density lost per unit time can be described as  $\frac{dw(t)}{dt} = w_0 (-\gamma) e^{-\gamma t}$ .

Suppose the average energy absorbed by free electrons is given as  $\langle \varepsilon_e \rangle = 2\pi m_e N_e \int_0^\infty v^2 f(v, t) dv$ , so the average energy absorbed per unit time can be derived as  $\frac{d\langle \varepsilon_e \rangle}{dt} = 2\pi m_e N_e \int_0^\infty v^2 \left( -\frac{\partial J(v)}{\partial v} \right) dv$ . According to the law of energy conservation, the laser power density lost per unit time is equal to the energy acquired by free electrons per unit time, i.e.

$$\frac{dw(t)}{dt} + \frac{d\langle \varepsilon_e \rangle}{dt} = 0. \quad (11)$$

Thus, the laser damping rate can be derived by solving Eq. (11):  $\gamma = \frac{8\pi N_e m_e}{\varepsilon_0 E_0^2} \int_0^\infty v J(v) dv$ , where  $J(v)$  is given by Eq. (7). For Gaussian pulses, the absorption coefficient at time  $t^*$  can be defined by  $\alpha_p(t^*) = \gamma t_p$ ;  $t_p$  is the pulse duration. This shows that the absorption coefficient is dependent on the

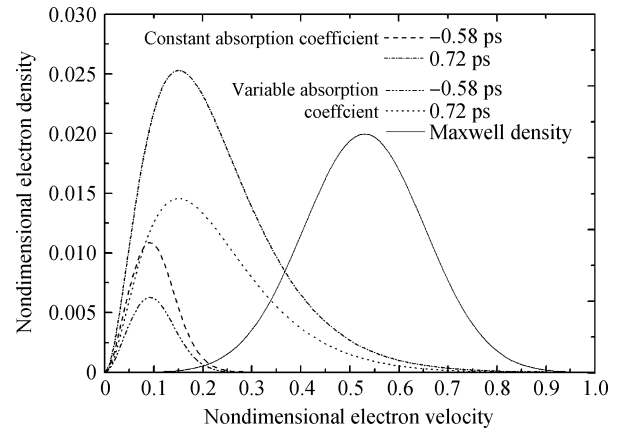


Fig. 1. Distribution functions of free electrons for 800 nm, 800 fs pulses with a peak intensity of  $8.5 \times 10^{13}$  W/cm<sup>2</sup>. Scenarios of constant and variable absorption coefficients, 0.58 and 0.72 ps, are included.

distribution functions of free electrons. The laser power density is expressed as  $I(t) = I_{\max}(1 - R) \exp \left[ -\alpha_p \left( \frac{t}{t_p} \right)^2 \right]$ .

#### 3.3. The relaxation time of free electrons

The relaxation time of free electrons in the conduction band transitioning from nonequilibrium to equilibrium can be described by the energy relaxation time, expressed as  $\tau_e^* = \frac{\langle \varepsilon^* \rangle}{\left| \frac{\partial \langle \varepsilon^* \rangle}{\partial t^*} \right|_{t^*=0}}$ , where  $\tau_e^*$  is the nondimensional relaxation time and  $\langle \varepsilon^* \rangle$  is the nondimensional average energy of free electrons given by  $\langle \varepsilon^* \rangle = \int_0^\infty v^{*2} f(v^*, t^*) dv^*$ .

### 4. Numerical calculation results

In this paper, a numerical simulation of the ablation of silica by femtosecond laser pulses is conducted. The physics parameters used in the simulation are listed in Table 1. Figure 1 displays the nondimensional distribution functions of free electrons for 800 nm, 800 fs pulses with a peak intensity of  $8.5 \times 10^{13}$  W/cm<sup>2</sup>. Several scenarios with different laser absorption coefficients are considered. The Maxwell distribution is plotted for comparison purposes. It can be seen that free electrons deviating from the Maxwell distribution are actually in a nonequilibrium state. It can also be observed from Fig. 1 that the number of high-energy free electrons is relatively low at the beginning of irradiation, but grows gradually during the irradiation process. It is also shown that at the same time, the number of free electrons with constant absorption coefficients is significantly less than pulses with variable absorption coefficients. This demonstrates that inverse bremsstrahlung absorption has a significant impact on the number density of free electrons in the conduction band.

Figure 2 illustrates the nondimensional time dependency of the nondimensional free electron density for 400 fs pulses of wavelengths with a peak intensity of  $8.5 \times 10^{13}$  W/cm<sup>2</sup>. It is observed that the free electron densities resulting from the pulses of variable absorption coefficients are considerably lower than those resulting from the pulses of constant absorp-

Table 1. Physical constants and laser parameters.

Name	Notation	Value	Unit
Electron number density of silica <sup>[26]</sup>	$N_e$	$8.22 \times 10^{28}$	$1/m^3$
Band gap energy <sup>[16]</sup>	$U_L$	9	eV
Electron charge <sup>[23]</sup>	$e$	$1.6 \times 10^{-19}$	C
Electron mass <sup>[23]</sup>	$m_e$	$9.11 \times 10^{-31}$	kg
Speed of light <sup>[23]</sup>	$C$	$3 \times 10^8$	m/s
Vacuum permittivity <sup>[23]</sup>	$\epsilon_0$	$8.9 \times 10^{-12}$	$C^2/N \cdot m^2$
Reduced Planck constant <sup>[23]</sup>	$\hbar$	$1.055 \times 10^{-34}$	J-s
Boltzmann coefficient <sup>[23]</sup>	$k_B$	$1.38 \times 10^{-23}$	J/K
Avalanche coefficient <sup>[24]</sup>	$\alpha$	$9.7 \times 10^{-4}$	$m^2/J$
Reflectivity <sup>[25]</sup>	$R$	0.945	

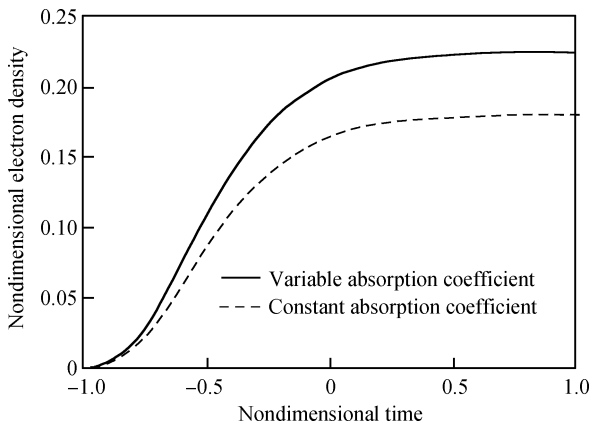


Fig. 2. Time dependence of free electron density for a 400 nm laser pulse with a peak intensity of  $8.5 \times 10^{13} \text{ W/cm}^2$ .

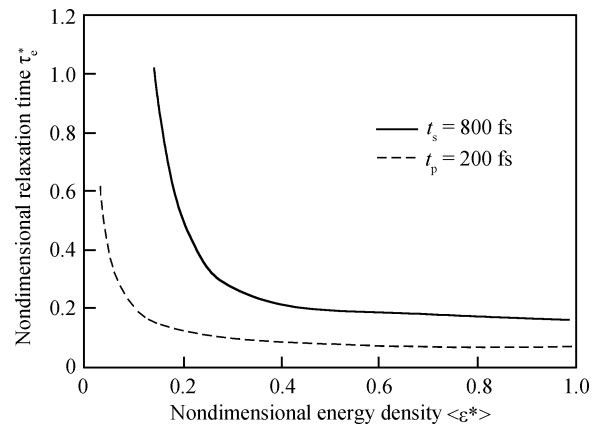


Fig. 4. Energy density dependence of the relaxation time for 800 nm pulses of 800 fs and 200 fs with a peak intensity of  $8.5 \times 10^{13} \text{ W/cm}^2$ .

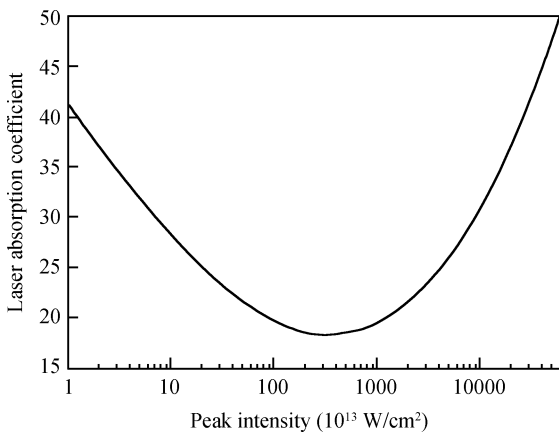


Fig. 3. Absorption coefficient as a function of laser peak intensity for 800 nm, 800 fs pulses at the start time ( $t^* = 0$ ).

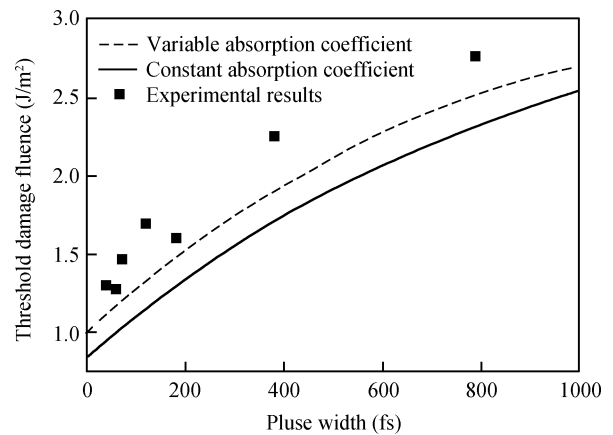


Fig. 5. Pulse width dependence of threshold damage fluence at 800 nm; the peak intensity is  $8.5 \times 10^{13} \text{ W/cm}^2$ .

tion coefficients at the same time; however, the differences gradually become stable as time elapses. This might be an explanation of the delay of ablation under the pulse irradiation of variable absorption coefficients.

Figure 3 depicts the absorption coefficient as a function of the laser peak intensity for 800 nm, 800 fs pulses at the start time ( $t^* = 0$ ). It is shown to be a concave function with the minimum value near the point of  $I_{MAX} = 10^{16} \text{ W/cm}^2$ , which is in agreement with the experimental results.

Figure 4 displays the nondimensional energy density de-

pendence of the nondimensional relaxation time for 800 nm pulses of 800 fs and 200 fs with the same peak intensity of  $8.5 \times 10^{13} \text{ W/cm}^2$ . It shows that the relaxation time of free electrons decreases as the energy density increases, and the relaxation time resulting from the 800 fs pulse is longer than that from the 200 fs pulse.

Figure 5 gives the pulse width dependence of the threshold damage fluence for a wavelength of 800 nm, with a peak intensity of  $8.5 \times 10^{13} \text{ W/cm}^2$ . Two scenarios, constant and variable absorption coefficients, are included. For comparison

purposes, the corresponding experimental results are also plotted. It can be seen that when the pulse duration is within the range of 200 fs, the computational results based on the developed model in this paper are obviously in better agreement with the experimental results than the constant absorption coefficient. And when the pulse duration is greater than the range of 200 fs, the computational accuracy of variable absorption coefficient is also better than the constant absorption coefficient. So the laser absorption coefficient is not a constant, and the laser absorption coefficient should be regarded as a variable parameter which is related to the free electron distribution.

## 5. Conclusions

In this paper, a nonlinear Fokker–Planck equation model is established to describe the time evolution of free electrons in the conduction band during the femtosecond laser ablation of semiconductors. Compared to the existing kinetics models in the literature, this model considers the impact of the mechanism of inverse bremsstrahlung absorption to the laser absorption coefficient. An iterative approach to effectively solve the Rosenbluth potential functions was presented. The computational results of the threshold damage fluences and laser absorption coefficients calculated are generally in good agreement with the experimental results, which indicates that the laser absorption coefficient should be regarded as a variable parameter for femtosecond pulsed lasers.

## References

- [1] Sun C K, Vallee F, Acioli L H, et al. Femtosecond-tunable measurement of electron thermalization in gold. *Phys Rev B*, 1994, 50: 15337
- [2] Fann W S, Storz R, Tom H W K, et al. Electron thermalization in gold. *Phys Rev B*, 1992, 46: 13592
- [3] Anisimov S I, Kapeliovich B L, Perelman T L. Electron emission from metal surfaces exposed to ultrashort laser pulses. *Sov Phys JETP*, 1974, 39: 375
- [4] Fujimoto J G, Liu J M, Ippen E P, et al. Femtosecond laser interaction with metallic tungsten and nonequilibrium electron and lattice temperatures. *Phys Rev Lett*, 1984, 53: 1837
- [5] Corkum P B, Brunel F, Sherman N K. Thermal response of metals to ultrashort-pulse laser excitation. *Phys Rev Lett*, 1988, 61: 2886
- [6] Chichkov B N, Momma C, Nolte S. Femto-second, picosecond and nanosecond laser ablation of solids. *Appl Phys A*, 1996, 63: 109
- [7] Lugovskoy A V, Bray I. Ultrafast electron dynamics in metals under laser irradiation. *Phys Rev B*, 1999, 60(5): 3279
- [8] Qiu T Q, Tien C L. Size effect on nonequilibrium laser heating of metal films. *J Heat Transfer*, 1993, 115: 842
- [9] Bejan D, Raseev G. Nonequilibrium electron distribution in metals. *Phys Rev B*, 1997, 55: 4250
- [10] Snoke D W, Wolfe J P. Population dynamics of a Bose gas near saturation. *Phys Rev B*, 1989, 39(7): 4030
- [11] Snoke D W, Rühle W W, Lu Y C, et al. Evolution of a nonthermal electron energy distribution in GaAs. *Phys Rev B*, 1992, 45(19): 10979
- [12] Fatti N D, Voisin C, Achermann M, et al. Nonequilibrium electron dynamics in noble metals. *Phys Rev B*, 2000, 61(24): 16956
- [13] Kaiser A, Rethfeld B, Vicanek M. Microscopic processes in dielectrics under irradiation by subpicosecond laser pulse. *Phys Rev B*, 2000, 61(17): 11437
- [14] Rethfeld B, Kaiser A, Vicanek M, et al. Ultrafast dynamics of nonequilibrium electrons in metals under femtosecond laser irradiation. *Phys Rev B*, 2002, 65: 214303
- [15] Rethfeld B. Unified model for the free-electron avalanche in laser-irradiated dielectrics. *Phys Rev Lett*, 2004, 92(18): 187401
- [16] Apostolova T, Hahn Y. Modeling of laser-induced breakdown in dielectrics with subpicosecond pulses. *J Appl Phys*, 2000, 88(2): 1024
- [17] Vatsya S R, Nikumb S K. Modeling of laser-induced avalanche in dielectrics. *J Appl Phys*, 2002, 91(1): 344
- [18] Stuart B C, Feit M D, Herman S, et al. Optical ablation by high-power short-pulse lasers. *J Opt Soc Am B*, 1996, 13(2): 459
- [19] Holway L H. Temporal behavior of electron distributions in an electric field. *Phys Rev Lett*, 1972, 28: 280
- [20] Keldysh L V. Diagram technique for nonequilibrium processes. *Zh Eksp Teor Fiz*, 1964, 47: 1515; Keldysh L V. *Sov Phys JETP*, 1965, 20: 1018
- [21] Lenzner M, Krüger J, Sartania S. Femtosecond optical breakdown in dielectrics. *Phys Rev Lett*, 1998, 80(18): 4076
- [22] Tien A C, Backus S, Kapteyn H, et al. Short-pulse laser damage in transparent materials as a function of pulse duration. *Phys Rev Lett*, 1999, 82: 3883
- [23] Woan G. *The Cambridge handbook of physics formulas*. Glasgow: University of Glasgow Press, 2000
- [24] Jia T Q, Xu Z Z, Li X X. Microscopic mechanisms of ablation and micromachining of dielectrics by using femtosecond lasers. *Phys Lett*, 2003, 82: 4382
- [25] Jasapara J, Nampoothiri A V V, Rudolph W, et al. Femtosecond laser pulse induced breakdown in dielectric thin films. *Phys Rev B*, 2001, 63: 045117